Available online at www.sciencedirect.com
SCIENCE DIRECT®
Surface Science 569 (2004) 185–192
SURFACE SCIENCE
www.elsevier.com/locate/susc

Submonolayer growth in the presence of defect sites

R. Vardavas *, C. Ratsch, R.E. Caflisch

Department of Mathematics, University of California, 520 Portola Plaza Math Sciences B, Los Angeles, CA 90095-1555, USA

Received 16 December 2003; accepted for publication 26 July 2004
Available online 20 August 2004

Abstract

Submonolayer epitaxy in the presence of defect sites on the substrate is studied by means of a level-set method. Here, island nucleations occur by the creation of dimers and defect-monomer pairs. We present results for the scaled island size distribution (ISD) for growth with different densities for both random and regularly positioned defects. The dynamics show that for large D/F and defect density, all islands are nucleated at the defect sites in the very early stages of growth. We use scaling ideas to show that a gamma distribution can suitably describe the ISD.

Keywords: Epitaxy; Growth; Surface defects

1. Introduction

Atomic defects on a substrate have long been known to affect nucleation during epitaxial growth. For many systems, defect sites act as traps for the diffusing adatoms [1–3]. An adatom and a defect can form the nucleus of an island that subsequently grows due to further aggregation. This acts as an important competing nucleation mechanism to islands formed by the creation of dimers, which occurs whenever two adatoms encounter and nucleate (we will refer to this as dimer nucleation). Islands grow at rates depending on their local environments, which in turn depend on their spatial distribution. Therefore, the location of defect sites has a strong influence on the growth dynamics. By controlling their positions it may be possible to obtain a desired surface morphology, so that they have practical technological applications. It is therefore of interest to know what submonolayer morphologies can be grown with different spatially distributed defect sites, from randomly to regularly positioned. Statistically, these grown morphologies are characterized by the scaled island size distribution (ISD).

Previous work in this field helps to give insight into the different possible ISDs that we can expect in the presence of defect sites. We first discuss models that do not explicitly include defect, but

* Corresponding author. Tel.: +1 3108254701; fax: +1 3102066673.
E-mail address: raffaello@vardavas.net (R. Vardavas).

0039-6028/$ - see front matter © 2004 Elsevier B.V. All rights reserved.
doi:10.1016/j.susc.2004.07.041

nevertheless are helpful to understand their effect. Models for "single atom nucleation" do not contain defect sites at the start of the evolution. Instead, the deposited adatoms have a constant probability to exchange with a substrate atom and thereby create a nucleation center or a defect site during the course of the evolution. These models have produced ISDs with very numerous small islands and exponentially decreasing larger islands [4,5]. An analytic treatment of related rate equations [6] for this model has indicated that in the scaling limit one obtains a constant ISD up to $s/\langle s\rangle < 2$. Random selection of nucleation centers has previously been investigated for dimer nucleation [7], producing a broad and nearly constant distribution of island sizes up to $s/\langle s\rangle = 1$. However, as we will explain below, this leads to different spatial correlations than islands that are nucleated at randomly distributed defect sites.

Growth models that explicitly include the defect sites have also been previously studied. In the scaling limit, a model by Mulheran and Blackman [8] has shown that the scaled ISD is a scaled gamma distribution with a shape parameter that is determined by the initial spatial arrangements of the defect sites. In their model, monomers were added sequentially into the system between defect-monomer nucleations, thereby suppressing any possibility for dimer nucleations. Furthermore, their investigation included a "hard disc exclusion zone", where the defects are never placed closer than a certain chosen area. The competition between dimer nucleation and defect-monomer pairs has been studied qualitatively by Lee and Barabási [9]. They presented a series of morphologies obtained for different growth condition over a substrate where the defect sites are regularly spaced. However, they did not show the ISDs obtained and they did not consider a more randomized set of defect site locations. Nouvertné et al. [10] observed that under certain growth conditions defect sites lead to bimodal growth. The reason is that defects-monomer pairs and dimers are nucleated at completely different stages in the growth. This results in two distinguished peaks in the ISD associated with the two nucleation mechanisms.

In this paper, we present results obtained by a level-set model that allows us to include nucleation through the formation of dimers and by defect-monomer pairs within the same framework. We present ISDs obtained for growths with both randomly and regularly distributed defect sites. We also find that in the scaling limit the scaled ISD is a scaled gamma distribution that is compared to that obtained in Ref. [8]. Furthermore, and unlike previous work, we show how the growth dynamics, in particular the evolution of the ISDs changes with different values of defect density and diffusion constant.

The level-set model provides certain advantages over other computational models like kinetic Monte Carlo. Here, we are not restricted to time steps associated with single adatom hops. The motion of the adatoms is modelled by evolving the continuous adatom density. This makes the model fast. Furthermore, the spatial and temporal fluctuations in island nucleation events is controlled by a set of rules applied to the adatom density field. These rules are easily modified, allowing more control over the growth dynamics. This in turn allows, for example, to investigate the importance of different forms of fluctuations [7]. We also note that other numerical schemes such as the phase-field model have been developed in the past few years to describe epitaxial growth [11]. However, we believe that the non-zero interface width of such models make them less amenable to the problems studied in the present paper.

2. The growth model

The level-set model for epitaxial growth [12–18], relies on the evolution of a continuous, spatially varying adatom density profile $\rho(\mathbf{x}, t)$ over the system. This determines the time and the position for the formation of new islands. It also relies on the level-set method for tracking the motion of the island boundaries. In this method a level-set function $\phi(\mathbf{x}, t)$ is used to describe the motion of the island boundary curves. These are represented by the sets of points for which $\phi(\mathbf{x}, t)$ takes integer values. For example, the set of boundary points that separate islands from the substrate satisfies $\phi(\mathbf{x}, t) = 0$ and is called the *zero-level-set*. The full time derivative of the level-set function yields an

advection equation that describes the motion of the points belonging to the island boundaries. This can be cast as

$$\frac{\partial \phi}{\partial t} + v_n \mid \nabla \phi \mid = 0, \tag{1}$$

where v_n is the velocity of the boundary in the outward normal direction $\mathbf{n} = \nabla\phi/|\nabla\phi|$. It is given by the net diffusion flow of the adatoms towards island steps edges. For the case of irreversible aggregation it is computed as

$$v_n = a^2 D \mathbf{n} \cdot [\nabla \rho^{\downarrow} - \nabla \rho^{\uparrow}], \tag{2}$$

where a is the lattice constant and $\nabla\rho^{\uparrow}$ and $\nabla\rho^{\downarrow}$ refer to the gradient of the adatom density evaluated above and below the island edge, respectively. The adatom density is obtained by numerically integrating the diffusion equation with the irreversible aggregation condition that $\rho = 0$ at island edges. In the presence of defect sites on the substrate, the diffusion equation can be written as

$$\frac{\partial \rho}{\partial t} = F + D\nabla^2 \rho - R_1 - 2R_2, \tag{3}$$

where R_1 and R_2 are the respective nucleation rates per site of defect-monomer pairs and dimers. The probability for two adatoms to be found at the same position and form a dimer is proportional to the local adatom density squared [7]. Therefore, we have that

$$R_2 = D\sigma_1 \rho^2, \tag{4}$$

where σ_1 is the adatom capture number. Similarly, the probability that an adatom is found at the same location as a defect site is proportional to both the local adatom density and the density of defect sites N_{def}° that have yet to absorb an adatom and form an island. Therefore, the rate for the nucleation of defect-monomer pairs can be expressed as

$$R_1 = D\sigma_1 N_{\mathrm{def}}^{\circ} \rho. \tag{5}$$

The adatom capture number that is used to compute the defect-monomer nucleation rate is the same as that for the dimer nucleation rate, since in our model a defect occupies one lattice site and acts like a stationary monomer. Our value for σ_1 is obtained by an expression [19] in terms of ρ that has been verified to correctly predict nucleation times by comparison to atomistic models [20,21].

The initial location of the defect sites are chosen at the beginning of each separate simulation and entered into a list. In this paper we consider both randomly and regularly placed defects. The number of defect sites placed is predetermined by the total defect density N_{def}. During growth, the density of available defect sites for nucleation is given by $N_{\mathrm{def}}^{\circ} = N_{\mathrm{def}} - N_{\mathrm{def}}^{\star}$, where $N_{\mathrm{def}}^{\star}$ is the density of islands that have been seeded at defect sites. Eqs. (1) and (3) are integrated between successive nucleation events. We determine when to nucleate a new island by separately tracking the time integrals of the spatial average of R_1 and R_2 over the entire system size L^2. When either of these two quantities increases above the next integer value, we respectively seed a new defect-monomer couple or a dimer. The location for a new dimer is determined by selecting a site with a probability proportional to its adatom density squared (cf. Eq. (4)). Similarly, the location for a new defect-monomer pair is randomly chosen from the list of the available defect sites with probabilities proportional to their local adatom density (cf. Eq. (5)). N_{def}° plays no role in selecting the defect site for nucleation since it does not have any spatial dependence and is constant between sucessive nucleations. A new island is then introduced into the system by raising the level-set function around a set of points centered at the selected nucleation site and this adds a new boundary curve to the zero-level-set. All the data presented in this paper were obtained for systems of size 180×180 sites over a square substrate, modelled by 512×512 grid sites. These were tested to give no system size effects. Depending on the initial defect density used our simulations were averaged over 10–100 independent runs.

3. Growth dynamics

The evolution of the island densities for D/F values of 10^4 and 10^7 with randomly placed defects with $N_{\mathrm{def}} = 0.01$ ML is shown in Fig. 1a. We see that for the smaller D/F value the total island density is larger than that of islands nucleated at the

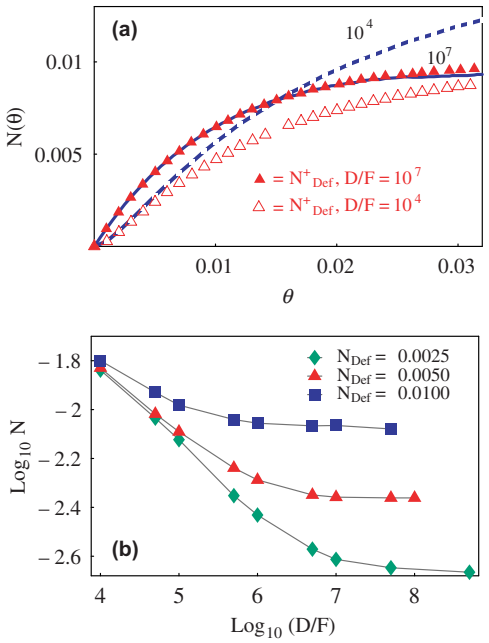

Fig. 1. (a) The evolution of the total island density (N) versus coverage (θ) for $D/F = 10^4$ and 10^7 is respectively shown by the dashed and solid lines for $N_{\text{def}} = 0.01$. The triangles show the associated evolutions of the density of occupied defect sites ($N^{\star}_{\text{def}}$) that have produced new islands. (b) A plot of the island density obtained at a coverage of 0.07 ML for different values of D/F for the initial defect densities of 0.0025, 0.005 and 0.01 ML.

defect sites, whereas for larger D/F value the density of island nucleated at defect sites and the total island density are nearly identical. In the latter, the typical length separating the defects is smaller than the characteristic adatom diffusion length that scales according to $l \sim (D/F)^{-1/6}$. As a result, dimer nucleation is completely suppressed. For low D/F, both dimers and defect sites are nucleated from the early stages of growth. The adatom diffusion length is comparable, or smaller than the typical lengths separating defect sites. Here, dimers continue to nucleate well past the stage where all defect sites produce an island seeding and the island saturation density is then entirely determined by the dimer nucleation rate. This can be clearly seen in the graph shown in Fig. 1b. At low values for D/F, dimer nucleation dominates and the island density drops according to $N \sim (D/F)^{-1/3}$. At high D/F values, the island density saturates to the initial defect density. This is consistent with the predictions obtained by the integration of rate equation that describe this type of growth as given in Ref. [1].

Typical surface morphologies obtained by evolving a system with the same set of randomly placed defects for two different values of D/F are shown in Fig. 2 at a coverage of 0.25 ML. For large D/F, all islands on the substrate are centered around defect sites. For low D/F, we see that islands are seeded at the same defect sites, and that in addition many other islands are formed by the creation of dimers. Also, due to the more prolonged nucleation of dimers, the variation in their island sizes is much larger than for those nucleated at defect sites. As can be seen by comparing the sample morphologies shown in Fig. 2, the relative variations of the capture zones are reduced for the larger D/F, where only defect sites get seeded.

The scaled ISD obtained for randomly positioned defects at a coverage of 0.25 ML is shown in Fig. 3. We find that the ISD obtained for a defect density of 0.01 ML (Fig. 3a) scales over a large set of values of D/F. The shape of this scaling distribution is noticeably different from the one previously obtained for "single atom nucleation" [4,5], which is characterized by a monotonic decrease in island densities with increasing island size. It is also different from the one obtained for just dimer nucleation with random seeding styles [7], where a near uniform ISD for island sizes $s/\langle s\rangle < 1$ has been found. Instead, the obtained ISD is much narrower and peaks slightly before $s/\langle s\rangle = 1$.

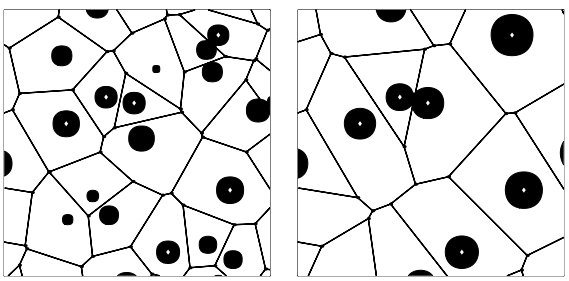

Fig. 2. Sample subregion of the morphologies obtained at 0.25 ML coverage for two similar systems containing the same set of defect sites evolved with $D/F = 5 \times 10^5$ (left) and 5×10^8 (right). The position of all defect sites are shown by white diamonds surrounded by their respective nucleated island (black). Also shown are the Voronoi cells associated to the island nucleation centers.

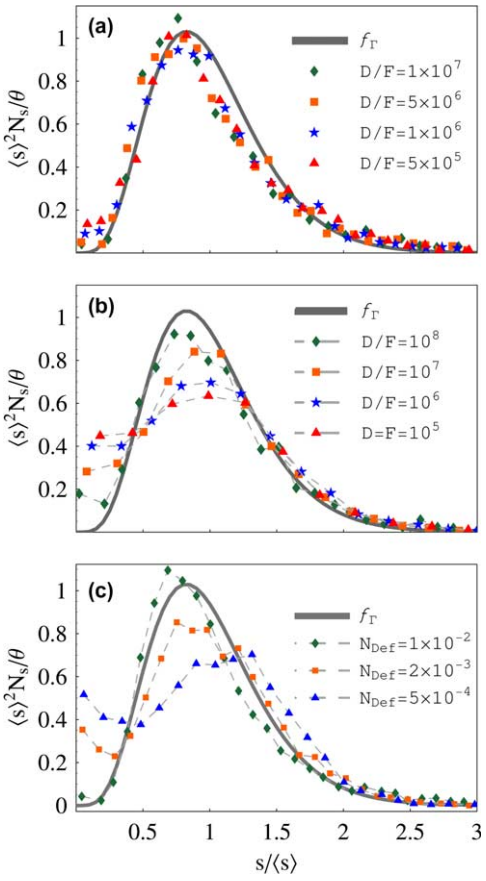

Fig. 3. Scaled ISD obtained at a coverage of $\theta = 0.25$ ML for different values of D/F, and for defect densities of 0.01 ML (a) and 0.0025 ML (b), and for different defect densities at constant $D/F = 10^7$ (c). N_s denotes the density of islands of size s and $\langle s \rangle$ denotes the average island size. Also shown is the analytic form of the scaled gamma distribution (f_Γ) given by Eq. (6) with $\kappa = 5.7$. The thin solid lines are a guide to the eye.

The reason why we get a peaked distribution even though the nucleation sites are random is largely due to the independence of the final island density on the growth parameters. As we have seen, once the defect density and the D/F values are large enough, a critical condition is reached where islands only nucleate at defect sites. These nucleations occur during the early stages of growth and the island density saturates. By further increasing D/F, islands are seeded at the same defect sites and the time intervals between successive nucleations decrease. The islands will therefore have approximately the same age, and variations in size result directly from the spatial variations in their growth environments. The above explanation was first suggested in Ref. [5]. In Fig. 3a, we see how little the form of the ISD changes, once we have reached the critical condition where all islands are nucleated at defect sites.

In the large D/F limit, the ISD approaches one that would be obtained if all defect sites were nucleated all together at time $t = 0$ (with no dimer nucleation). The ISD approaches a form similar to that for the spatial distribution of the capture zone areas [16] of the growing islands. Therefore, we can approximate the capture zone area distribution during growth by the initial capture zones, that are defined by the defect sites. The problem is then reduced to the geometric computation of the distribution of Voronoi cell areas associated to points, that represent the defects placed randomly over a flat two dimensional periodic surface. This follows a gamma distribution [8] with a mean set to unity, and has the following general form

$$f_\Gamma(x,\kappa) = \kappa \frac{(\kappa x)^{\kappa-1} e^{-\kappa x}}{\Gamma(\kappa)}, \tag{6}$$

where κ is the shape parameter. The distribution of the areas associated with the cells of a Voronoi tessalation around randomly placed points follows a gamma distribution with shape parameter $\kappa = 3.61$ [22]. By knowing the form of the distribution of the capture zone areas that are associated with the defect sites, we can compute the form of the ISD for D/F values large enough such that only defect-monomer pairs nucleate. This is done by convolving the capture zone area distribution to the homogenous Poisson point process distribution, which is associated with shot noise fluctuations in the nucleation events of the different defect sites [23].

The form of the ISDs in Fig. 3a is closer to a more peaked gamma distribution than that obtained with a shape parameter of 3.61. We can compare the limiting form of this ISD to one obtained when all islands are nucleated in infinitesimally short intervals. For simplicity, we may assume a special case where all islands are nucleated at the defect sites at $t = 0$. This is referred to

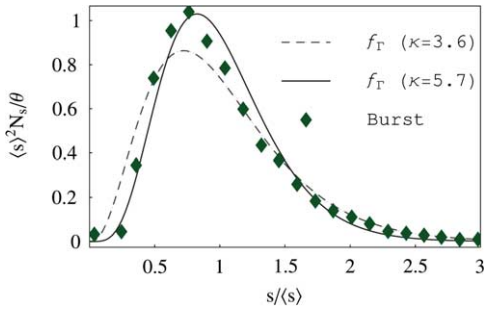

Fig. 4. Scaled ISD obtain for the growth when islands of size 1 are seeded at all the defect sites at time $t = 0$ in a *burst of nucleation* (see discussion in the text), and are allowed to evolve with $D/F = 10^6$. Gamma distributions with shape parameter $\kappa = 5.7$ and 3.61 are shown.

as a burst of nucleation. The scaled ISD for this special case is shown in Fig. 4. We see that the ISD is best approximated by a gamma distribution with shape parameter $\kappa = 5.7$. This is the same gamma distribution that is shown together with the data in the Fig. 3. We believe that the reason for a larger shape parameter is mainly due to the initial size of the nucleated dimers that makes the ISD at the initial burst of nucleation a delta function. [1] The island sizes then evolve according to their capture zone areas and thus the ISD relaxes towards the capture zone areas gamma distribution. [2]

For a lower defect density of 0.0025 ML, the ISD shown in Fig. 3b changes form significantly, as we increase D/F. In the high D/F limit, the only islands seeded are at defect sites. The shape of the ISD adjusts by making small alterations and eventually the same scaled gamma distribution is reached as shown in Fig. 3a. For lower D/F values, defect-monomer pairs and dimers have comparable nucleation frequencies. Here, the location of island centers are chosen by two very different ways and their nucleation time series overlap. By making even small variations to D/F, we change the weights or the relation between one spatial fluctuation in island nucleation with respect to the other. As we further decrease D/F, we increase the frequency of dimer nucleations with respect to defect-monomer nucleation, and obtain many more islands. So even though all defect sites give rise to an island seeding, there are many more islands nucleated by dimers. Therefore, the defect sites have a smaller impact on the growth. It can be seen in Fig. 3b (triangles) that in this limit the form of the ISD approaches the one obtained with only dimer nucleations. [3]

The transition from predominant dimer nucleation to defect nucleation can also be seen in the ISDs observed for a fixed D/F and increasing defect density. Fig. 3c shows the ISDs obtained for the growth with $D/F = 10^7$ at various defect densities. Again we notice a big change in the form of the ISD going from a low to a high defect density. The ISD for the lowest defect density of 0.0005 ML differs very little from that obtain with just dimer nucleation. In contrast, the ISD for high defect densities of 0.01 and 0.005 ML is similar to the gamma distribution with $\kappa = 5.7$. However, all of the ISDs fall off in the same way as these large islands correspond to the earliest nucleations.

We now turn our discussion from the more common scenario where the location of defect sites are random to the technologically more desirable

[1] We speculate that in the unphysical limit where the capture zone areas are much larger that the defect-monomer size our ISDs would still be a gamma distribution but with a shape parameter smaller than 5.7.

[2] We note that in Ref. [8], the data obtained for the ISD followed an even more peaked gamma distribution. Our understanding is that this is due to a controllable parameter used in their model that forces defects to be no closer than a minimum length. The introduction of what they call the "hard-disc exclusion condition" modifies the true randomness of the defect sites, and delays coalescence. In fact, our results for regularly distributed defects (see below) show that less randomness leads to a sharper ISD (and thus, a larger shape parameter).

[3] We note an additional effect that reduces the importance of defect nucleation in this limit: for very low D/F, the adatom density during the early stages of growth does not evolve very fast between sucessive nucleation events. This results in a large central region where the adatom density stays approximately uniform between island boundaries. Here, the difference between the ρ^2 weighting in the selection of the new location of a nucleated dimer and a random selection is negligable. Therefore, at very low D/F early dimer nucleations share similar random fluctuations in nucleation sites as defect-monomer pairs. This makes the presence of the randomly located defects unimportant to the overall spatial fluctuations in the island environments since their nucleation occurs during this stage of growth.

one where they are arranged in a regular array. The ISD obtained for regularly placed defect sites that are arranged over the substrate such that each contains the same capture zone area is shown in Fig. 5a for an initial defect density of 0.01 ML. The form of the ISD is clearly very narrow and highly peaked (note the scale of the y-axis in comparison to Fig. 3). Due to the regularity of the defect sites, the average adatom density will be small, thus further reducing the dimer nucleation which for $D/F \sim 10^5$ becomes a rare event and is completely suppressed for larger values. The ISD is then entirely controlled by the time series for defect monomer nucleation. In the large D/F limit the ISD approaches a distribution obtained by convolving the Poisson distribution associated to the fluctuations in nucleation events with the delta function distribution of the capture areas. This limiting distribution is well approximated by a highly peaked gamma distribution. A gamma distribution with shape parameter equal to the number of defects sites is also shown in Fig. 5a.

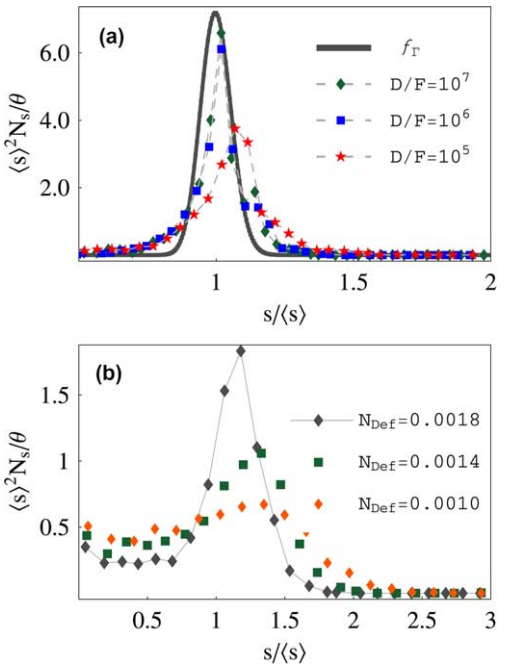

Fig. 5. Scaled ISD at $\theta = 0.25$ ML for regularly positioned defects sites with density 0.01 ML (a) grown at D/F values of 10^5, 10^6 and 10^7. Also shown is the analytic form of the scaled gamma distribution given by Eq. (6) with $\kappa = 324$. The ISDs shown in panel (b) illustrate the dramatic change in the form of the ISD for growths at constant $D/F = 10^7$ and defect densities in the range of 0.001–0.0018. The thin solid lines are a guide to the eye.

Fig. 5b shows the change in the shape of the ISD over a small range of defect densities at a constant $D/F = 10^7$. For a defect density of 0.001 ML and a coverage of 0.25 ML we observe that the number of nucleated islands is approximately twice the number of defect sites. This turns out to be sufficient for obtaining an ISD that has a form which resembles the one with just dimer nucleation. This can be seen by comparing the ISDs obtained at the defect density of 0.001 ML for randomly distributed defects (Fig. 3c) and that for regularly distributed defects. However, as we increase the defect density to 0.0018 ML, there is a very noticeable change in the ISD. Here, the island density has nearly reached the saturation density, where all islands were nucleated by a defect-monomer.

Growth with regularly placed defects produces islands that have similar shapes and sizes as it has been previously observed in Ref. [9] via kinetic Monte Carlo simulations. Lee and Barabási illustrated how the surface morphology changes as the flux is varied for growths with constant temperature and defect density. However, they did not show plots of the related ISDs and how they change form by varying both D/F and defect density. In this paper we demonstrate that regularly placed defects indeed lead to a narrowing of the ISD and how it changes over different growth conditions. If it is the goal to grow islands with the same shape and size, then we found that this is best achieved at the highest possible D/F. However, at large temperatures reversibility might become an important effect. Although our level-set model can consider reversibility in the growth of islands [24], this investigation is beyond the scope of this paper. Once all the defect sites are nucleated and the adatom density falls close to its equilibrium value, the islands will begin to ripen where large islands gain more mass at the expense of detachment from the smaller ones. This would lead to a bimodal ISD. Lee and Barabási therefore suggested that an "optimal flux" exists such that the diffusion length is approximately the same as the

length separating adjacent defects. However, in light of our results we can conclude that this depends on how important ripening and reversibility are during growth.

4. Conclusion

In summary, defect sites are nucleated very early in the growth. As a result, for large defect densities and large D/F, dimer nucleation is completely suppressed and islands grow according to the spatial distribution of the defect sites. This produces peaked ISDs that can be approximated by scaled gamma functions with increasing shape parameter as one goes from a random to a regular distribution of the defect sites. These results suggest that they can be used for many technological applications. An example would be in the growth of self assembled quantum dots, whereby one wants to produce a coherent array of islands, each acting as local single electron quantum confinement centers. These quantum dots serve for example as a resonant tunneling transistors, performing the function of several conventional transistors. Recent experimental results by Alchalabi et al. [25] have shown that the growth of uniformly sized quantum dots can be due to the presence of a regular array of dislocation sites. Their results and the explanation they provide is in very good agreement with the ideas presented in this paper.

References

[1] J.H. Harding, A.M. Stoneham, J.A. Venables, Phys. Rev. B 57 (1997) 6715.
[2] J.A. Venables, J.H. Harding, J. Crystal Growth 211 (2000) 27.
[3] G. Haas, A. Menck, H. Brune, J.V. Barth, J.A. Venables, K. Kern, Phys. Rev. B 61 (2000) 11105.
[4] D.D. Chambliss, K.E. Johnson, Phys. Rev. B 50 (1994) 5012.
[5] A. Zangwill, E. Kaxiras, Surf. Sci. 326 (1995) L483.
[6] D.D. Vvedensky, Phys. Rev. B 62 (2000) 15435.
[7] C. Ratsch, M.F. Gyure, S. Chen, M. Kang, D.D. Vvedensky, Phys. Rev. B 61 (2000) R10598.
[8] P.A. Mulheran, J.A. Blackman, Philos. Mag. Lett. 72 (1) (1995) 55.
[9] C. Lee, A.L. Barabási, Appl. Phys. Lett. 73 (1998) 2651.
[10] F. Nouvertné, U. May, M. Bamming, A. Rampe, U. Korte, G. Güntherodt, R. Pentcheva, M. Scheffler, Phys. Rev. B 60 (1999) 14382.
[11] A. Karma, M. Plapp, Phys. Rev. Lett. 81 (1998) 4444.
[12] R.E. Caflisch, M.F. Gyure, B. Merriman, S. Osher, C. Ratsch, D.D. Vvedensky, J.J. Zinck, Appl. Math. Lett. 12 (1999) 13.
[13] M.F. Gyure, C. Ratsch, B. Merriman, R.E. Caflisch, S. Osher, J.J. Zinck, D.D. Vvedensky, Phys. Rev. E 58 (1998) R6927.
[14] S. Chen, M. Kang, B. Merriman, R.E. Caflisch, C. Ratsch, R. Fedkiw, M. Gyure, S. Osher, J. Comp. Phys. 167 (2001) 475.
[15] C. Ratsch, M.F. Gyure, R.E. Caflisch, F. Gibou, M. Petersen, M. Kang, J. Garcia, D.D. Vvedensky, Phys. Rev. B 65 (2002) 195403.
[16] M.C. Bartelt, J.W. Evans, Phys. Rev. B 54 (1996).
[17] J.A. Blackman, P.A. Mulheran, Phys. Rev. B 54 (1996).
[18] J.W. Evans, M.C. Bartelt, Phys. Rev. B 66 (2002) 235410.
[19] J.A. Venables, Philos. Mag. B 27 (1973) 697.
[20] G.S. Bales, D.C. Chrzan, Phys. Rev. B 50 (1994) 6057.
[21] G.S. Bales, Surf. Sci. 356 (1995) L439.
[22] D.L. Weaire, J.P. Kermode, J. Wejchert, Philos. Mag. B 53 (1986) L101.
[23] V. Fournée, A.R. Ross, T.A. Lograsso, J.W. Evans, P.A. Thiel, Surf. Sci. 537 (2003) 5.
[24] M. Petersen, C. Ratsch, R.E. Caflisch, A. Zangwill, Rev. E 64 (2001) 061602.
[25] K. Alchalabi, D. Zimin, G. Kostorz, H. Zogg, Phys. Rev. Lett. 90 (2003) 026104.